

Dalton Transactions

Accepted Manuscript



This is an *Accepted Manuscript*, which has been through the Royal Society of Chemistry peer review process and has been accepted for publication.

Accepted Manuscripts are published online shortly after acceptance, before technical editing, formatting and proof reading. Using this free service, authors can make their results available to the community, in citable form, before we publish the edited article. We will replace this *Accepted Manuscript* with the edited and formatted *Advance Article* as soon as it is available.

You can find more information about *Accepted Manuscripts* in the [Information for Authors](#).

Please note that technical editing may introduce minor changes to the text and/or graphics, which may alter content. The journal's standard [Terms & Conditions](#) and the [Ethical guidelines](#) still apply. In no event shall the Royal Society of Chemistry be held responsible for any errors or omissions in this *Accepted Manuscript* or any consequences arising from the use of any information it contains.

Slow magnetic relaxation in mononuclear seven-coordinate cobalt(II) complexes with easy plane anisotropy

Lei Chen,^a Shu-Yang Chen,^a Yi-Chen Sun,^b Yu-Mei Guo,^b Lu Yu,^c Xue-Tai Chen,^{*a} Zhenxing Wang,^b Z. W. Ouyang,^b You Song,^a and Zi-Ling Xue^d

Abstract: Two mononuclear seven-coordinate cobalt(II) complexes [Co(L)₃(NO₃)₂] (L = 4-*tert*-butylpyridine, **1**; L = isoquinoline, **2**) were prepared and structurally analyzed by single-crystal X-ray crystallography. The coordination spheres of **1** and **2** exhibit the distorted pentagonal bipyramid geometry. Analysis of their direct-current magnetic data reveals the existence of easy plane anisotropy ($D > 0$) with small transverse anisotropy (E), which was further confirmed by high-field electron paramagnetic resonance (HFEP) spectroscopy. Field-induced slow magnetic relaxations were observed under the applied dc field in complexes **1** and **2** by alternating-current magnetic susceptibility measurements. Importantly, these complexes constitute new instances of mononuclear high-coordinate cobalt(II)-based single-molecule magnets.

^aState Key Laboratory of Coordination Chemistry, Nanjing National Laboratory of Microstructures, School of Chemistry and Chemical Engineering, Nanjing University, Nanjing 210093, China. E-mail:

xtchen@netra.nju.edu.cn; Fax: +86 25 83314502

^bWuhan National High Magnetic Field Center, Huazhong University of Science and Technology, Wuhan 430074, China

^cHigh Magnetic Field Laboratory, Hefei Institutes of Physical Science, Chinese Academy of Sciences, Hefei 230031, China

^dDepartment of Chemistry, University of Tennessee, Knoxville, Tennessee 37996, USA.

† Electronic supplementary information (ESI) available: Detailed crystallographical data, XRD patterns, and magnetic data.

Introduction

In the past two decades, single-molecule magnets (SMMs), which are based on the intrinsic properties of individual molecules rather than the interactions between molecules, have invoked much research interest, providing excellent model systems for understanding the quantum effects and offering unprecedented potential applications in high-density spin-based information storage and processing, quantum computation, and spintronics.¹ Studies of the SMM behavior have been focused on transition metal clusters² and those containing lanthanide ions.³ More recently, the research effort was turned to the smaller molecules like mononuclear Ln(III)⁴ and transition metal complexes,⁵⁻¹⁰ which have been called as single-ion magnets (SIMs). The local magnetic anisotropy and the resulting SIM properties may be fine-tuned by variation of the ligand field. It is believed that the low coordination environment for first-row transition metal complexes form a relatively weak ligand field resulting in the d orbital energy splitting with a small separation between the electronic ground state and the excited states, thus maximizing the spin-orbit coupling to enhance the magnetic anisotropy.^{11,12} Indeed, the two-coordinate Fe(I) complex [K(crypt-222)][Fe(C(SiMe₃)₃)₂] showed the largest yet effective spin-reversal barrier of $U_{eff} = 226(4) \text{ cm}^{-1}$ for SMMs based on pure transition metal.^{7a} So far Co(II)-based SIMs are the most extensively studied family among the transition metal ion SIMs with which coordination number ranging from two to six and a variety of coordination geometries including trigonal-planar, tetrahedral, square-pyramidal, triangular prism and octahedral polyhedron with different distortions.⁵⁻⁶ Recently we reasoned that the

high coordination geometry may also lead to a small energy separation between the electronic spin ground state and low-lying excited state if the donor atoms provide a weak coordination field. We have reported the first eight-coordinate Co(II)-containing SIM exhibiting field-induced slow relaxation of magnetization, in which Co(II) ion is sandwiched by two 12-crown-4 ligands, generating the large and negative magnetic anisotropy with the zero-field splitting parameter D value of -37.6 cm^{-1} .⁶⁰ Huang *et al* revealed the slow magnetic relaxation in three mononuclear seven-coordinate Co(II) complexes with pentagonal bipyramid geometry supported by pentadentate ligand^{5j}. Due to the limited number of the high-coordinate Co(II)-based SIMs compared to a great number of low-coordination analogues, the dynamic magnetic properties of mononuclear Co(II) complexes with the high-coordination number (seven or eight) are worthy of further exploration in search for new SIMs and investigation of the relationship between the magnetic anisotropy and ligand field.

As part of our research into the high-coordinated transition metal ion SIMs and their dynamic magnetic properties, herein we report structural characterization and the magnetic properties of two seven-coordinate mononuclear cobalt(II) complexes $[\text{Co}(\text{L})_3(\text{NO}_3)_2]$ ($\text{L} = 4\text{-tert-butylpyridine}$, **1**; $\text{L} = \text{isoquinoline}$, **2**). Both complexes display field-induced slow magnetic relaxation behavior with the zero-field splitting parameter $D > 0$. It is noted that the coordination spheres of our compounds exhibit more serious distortion of pentagonal bipyramid geometries due to the occurrence of an unsymmetrical binding NO_3^- group compared with the reported seven-coordinate Co(II)-SIMs.^{5j}

Experimental Section

General considerations

All manipulations were carried out using standard Schlenk techniques under nitrogen atmosphere. Solvents were dried over molecular sieves and distilled under nitrogen. Unless otherwise stated, all chemicals were purchased from commercial sources and used without further purification. Elemental analyses were performed on an Elementar Vario ELIII elemental analyzer. The powder XRD patterns were recorded at room temperature on a BRUKER D8 ADVANCE X-ray diffractometer. Inductively coupled plasma-optical emission spectrometry (ICP OES-Optima 5300DV, Perkinelmer Inc., Waltham, MA, USA) was employed to confirm the ratio of Zn:Co in the diluted sample.

Synthesis of $[\text{Co}(\text{L})_3(\text{NO}_3)_2]$ (L = 4-*tert*-butylpyridine, **1**)

To a solution of CoCl_2 (1.0 mmol, 0.13 g) in 10.0 mL acetonitrile was added a solution of AgNO_3 (2.0 mmol, 0.34 g) in 10 mL acetonitrile. The mixture was stirred until the reaction was complete, then the insoluble silver chloride was removed by filtration. 4-Tert-butylpyridine (3.4 mmol, 0.5 mL) was slowly added to the filtrate, and the solution was allowed to stand overnight. The red brown block crystals were isolated in 85% yield based on Co content. Elemental analysis (%) calcd. for $\text{CoC}_{27}\text{N}_5\text{O}_6\text{H}_{39}$ (MW 588.6): C, 55.10; H, 6.68; N, 11.90. Found: C, 55.20; H, 6.68; N, 11.69.

Synthesis of [Co(L)₃(NO₃)₂] (L = isoquinoline, 2)

Compound **2** was prepared by the same procedure as compound **1**, but with isoquinoline (3.4 mmol, 0.4 mL) used instead of 4-*tert*-butylpyridine (3.4 mmol, 0.5 mL). The deep red brown block crystals were isolated in 80% yield based on Co content. Elemental analysis (%) calcd. for CoC₂₇N₅O₆H₂₁ (MW 570.4): C, 56.85; H, 3.71; N, 12.28. Found: C, 56.55; H, 3.84; N, 11.91.

Synthesis of [Co_{0.1}Zn_{0.9}(L)₃(NO₃)₂] (L = 4-*tert*-butylpyridine, Zn-1)

The diluted sample **Zn-1** was prepared by the same procedure as compound **1**, but with the mixture of CoCl₂ (0.1 mmol, 0.013 g) and ZnCl₂ (0.9 mmol, 0.123 g) used instead of CoCl₂ (1.0 mmol, 0.13 g). The red microcrystal was isolated in 76% yield based on Co content. Successful dilution was confirmed by XRD and ICP OES data.

X-ray Structure Determination

X-ray diffraction data for **1** and **2** were collected using a Bruker APEX DUO diffractometer with a CCD area detector (Mo K α radiation, $\lambda = 0.71073$ Å) at room temperature.¹³ The APEXII program was used for collecting frames of data, determining lattice parameters. Data were integrated through the SAINT. Absorption corrections were applied using SADABS.¹⁴ The structures were solved using SHELXS-97 and subsequently completed by Fourier recycling using SHELXL 97 program.¹⁵ The Co atoms were firstly determined, and O, N and C atoms were subsequently identified by the difference Fourier maps. All non-hydrogen atoms were

refined by anisotropic displacement parameters. Hydrogen atoms on organic ligands were set in the calculated positions and generated by the riding model.

Crystallographic data, data collection, and refinement parameters for **1** and **2** are listed in Table S1 in the ESI.

Magnetic measurements

Magnetic susceptibility measurements were recorded with a Quantum Design SQUID VSM magnetometer. Direct current susceptibility data were collected between 1.8 and 300 K using an applied field of 1.0 kOe. Magnetization measurements were performed from 1.8 to 5 K at fields up to 7.0 T. The temperature and frequency-dependent alternative-current susceptibility data were collected using an oscillating ac field of 2.0 Oe at ac frequencies ranging from 1 to 1000 Hz. The magnetic susceptibilities data were corrected for the sample holder, as well as for diamagnetism of the constituent atoms (estimated using Pascal's constants). HF EPR measurements were performed on a locally developed spectrometer at Wuhan National High Magnetic Field Center, using a pulsed magnetic field of up to 30 T.¹⁶ The X-band ($f = 9.36$ GHz) low-field electron spin resonance (ESR) measurements were carried out at High Magnetic Field Laboratory of the Chinese Academy of Sciences, using a Bruker EMX plus 10/12 CW-spectrometer, equipped with a continuous He gas-flow cryostat to cover the temperature range 1.8–300 K.

Results and discussion

The molecular structures of **1** and **2** were characterized by the single-crystal X-ray

diffraction analyses, which are presented in Figure 1. The selected bond distances and angles around the cobalt (II) ion are listed in Table 1. As shown in Figure 1, complexes **1** and **2** possess the pentagonal bipyramid geometry. In **1**, the central cobalt atom is coordinated by three 4-*tert*-butylpyridine and two bidentate NO₃⁻ groups. The axial sites are occupied by two nitrogen atoms of 4-*tert*-butylpyridine, while the equatorial plane is formed by four oxygen atoms (O1, O2, O4, O5) from the two bidentate NO₃⁻ groups and one nitrogen atom (N1) from 4-*tert*-butylpyridine. One of the NO₃⁻ groups binds in unsymmetrical bidentate mode¹⁷ resulting in a shorter Co–O distance (Co–O(1)) of 2.138(4) Å and a longer one (Co–O(2)) of 2.509(6) Å. However, the other NO₃⁻ group coordinated to Co(II) ion in a more symmetrical fashion with the small discrepancy between Co–O distances of about 0.1 Å. The distances of Co–N(1), Co–N(2) and Co–N(3) bonds are 2.145(4), 2.163(4) and 2.170(4) Å, respectively. The equatorial O–Co–O angle in the interior of NO₃⁻ groups [56.32(16)° and 52.70(16)°] are significantly smaller than the other three equatorial bond angles N(1)–Co–O(1) [87.93(16)°], N(1)–Co–O(4) [85.92(17)°] and O(2)–Co–O(5) [77.2(2)°]. All of them deviate seriously from the angle for an ideal pentagonal bipyramid (72°). The axial N–Co–N bond angle (171.89(16)°) is also close to linearity for an ideal pentagonal bipyramid. The structural feature of **2** is similar to that of **1**, as depicted in Figure 1 with the structural parameters listed in Table 1. We have also performed the continuous shape measurement (CShM) analysis by SHAPE 2.1 program.¹⁸ The values of 1.410 and 1.542 obtained for **1** and **2** relative to the ideal pentagonal bipyramid, respectively, support the small distorted deviations. The

shortest intermolecular Co–Co distances for complexes **1** and **2** are 6.722 and 6.898 Å, respectively.

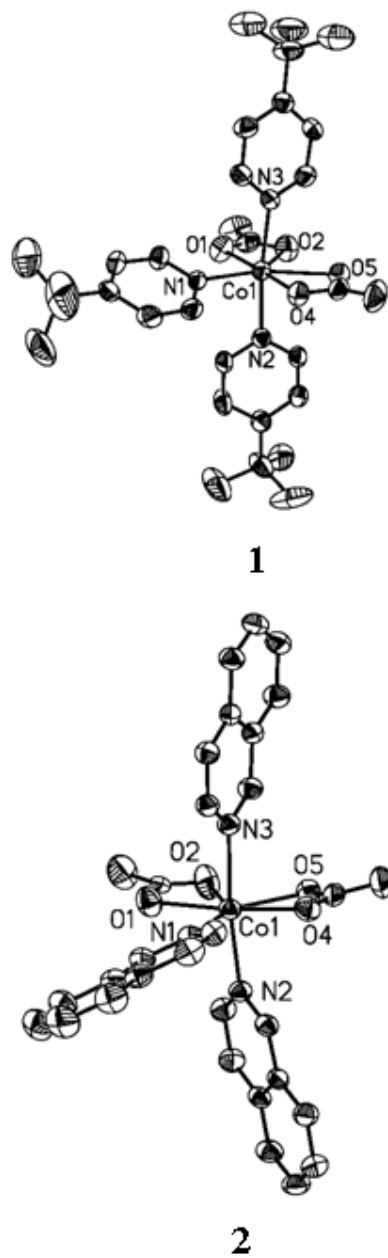


Figure 1. Structures of complexes **1** and **2**. H atoms are omitted for clarity.

Table 1. Selected Bond Lengths (Å) and Angles (deg) for **1** and **2**.

	1	2
Co(1)-O(1)	2.138(4)	2.169(2)
Co(1)-O(2)	2.509(6)	2.400(3)
Co(1)-O(4)	2.183(4)	2.205(2)
Co(1)-O(5)	2.284(4)	2.232(2)
Co(1)-N(1)	2.145(4)	2.148(2)
Co(1)-N(2)	2.163(4)	2.141(2)
Co(1)-N(3)	2.170(4)	2.154(2)
N(1)-Co(1)-O(1)	85.92(17)	84.74(9)
N(1)-Co(1)-O(4)	87.93(16)	89.72(8)
O(4)-Co(1)-O(5)	56.32(16)	57.46(8)
O(1)-Co(1)-O(2)	52.70(19)	53.78(8)
O(2)-Co(1)-O(5)	77.2(2)	74.77(8)
N(2)-Co(1)-N(3)	171.89(16)	172.64(8)

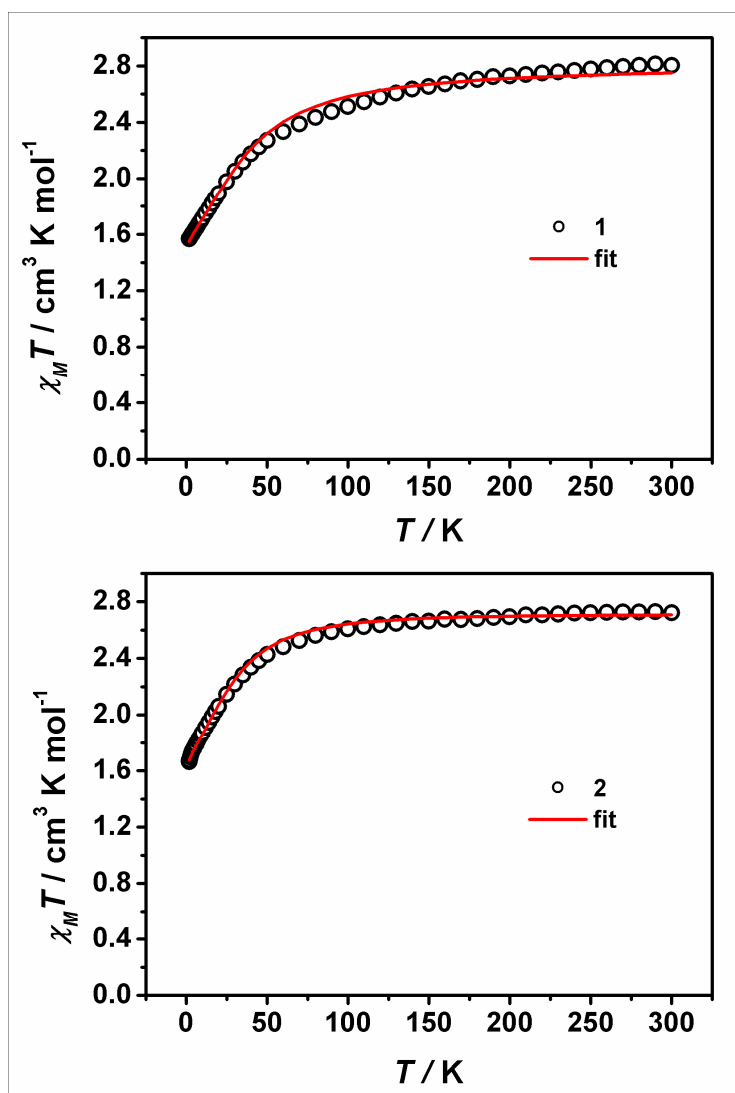


Figure 2. Variable-temperature dc susceptibility data of polycrystalline samples of **1** and **2**. Solid red lines indicate the best fits with the *PHI* program.¹⁹

Direct-current (dc) magnetic susceptibilities were measured for **1** and **2** in the temperature range 1.8–300 K. The two complexes show similar magnetic behavior (Figure 2). At 300 K, the $\chi_M T$ values are 2.80 and 2.72 $\text{cm}^3 \text{K mol}^{-1}$ for **1** and **2**, respectively, which are larger than the expected spin-only value of 1.875 $\text{cm}^3 \text{K mol}^{-1}$ for mononuclear cobalt(II) ion ($S = 3/2$, $g = 2.0$). Upon cooling, the $\chi_M T$ products for **1**

and **2** gradually decrease to about 50 K, after which they rapidly decrease to the minimum values of 1.57 and 1.66 at $\text{cm}^3 \text{K mol}^{-1}$ at 1.8 K, respectively. The downturn below 50 K is attributed to the effect of magnetic anisotropy of the cobalt(II) ion rather than intermolecular interactions due to the long distances between the Co(II) ions. The magnetizations were measured from 0 to 7 T at different temperatures, as shown in Figure 3. With the magnetic field increases, the magnetizations continuously rise to reach 2.22 and 2.30 $N\beta$ at 7 kOe for **1** and **2**, respectively. The high-field non-saturation and the non-superposition of M versus H/T curves (Figure 3) suggest the presence of significant magnetic anisotropies in **1** and **2**.

In order to get the insight into the magnetic anisotropy, the trustworthy ZFS parameters were obtained by simultaneously fitting the $\chi_M T$ versus T and the M versus H/T curves using the *PHI* program,¹⁹ that diagonalizes an anisotropic spin Hamiltonian. The parameters of D , E , and g were selected to correlate the data. In the fit process, it was found that the fitting results were insensitive to the initial values of the parameters E and g , while the sign of the initial D value is crucial to the final fitting result. Only when the sign of the initial parameter D was assigned to be positive, the reasonable results were obtained. The best fit values were summarized in Table 2, which reveals the anisotropic g parameters, large and positive D values and small E values for **1** and **2**. Similar large and positive D values from +25 to +33 cm^{-1} have been reported for the seven-coordinate Co(II) complexes with pentagonal bipyramid geometry, in which a pentadentate ligand is located in the equatorial positions.^{5j,20}

Table 2. The fitting results of the magnetization data by the *PHI* program¹⁹ for complexes **1** and **2**.

	$g_{x,y}$	g_z	$D(\text{cm}^{-1})$	$ E (\text{cm}^{-1})$	Residual
1	2.26	2.78	35.8	0.21	0.000063
2	2.43	2.35	35.7	0.02	0.000029

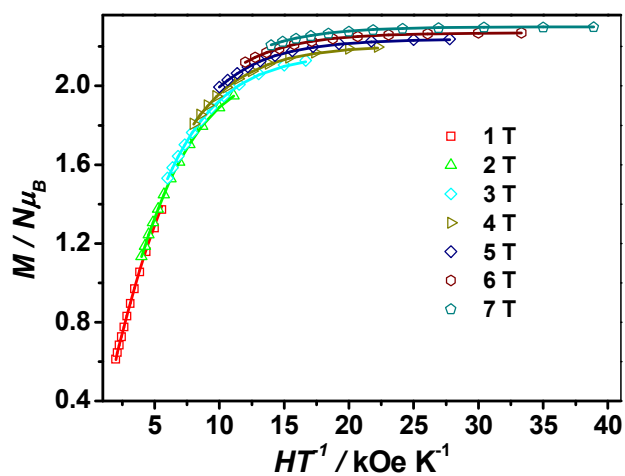
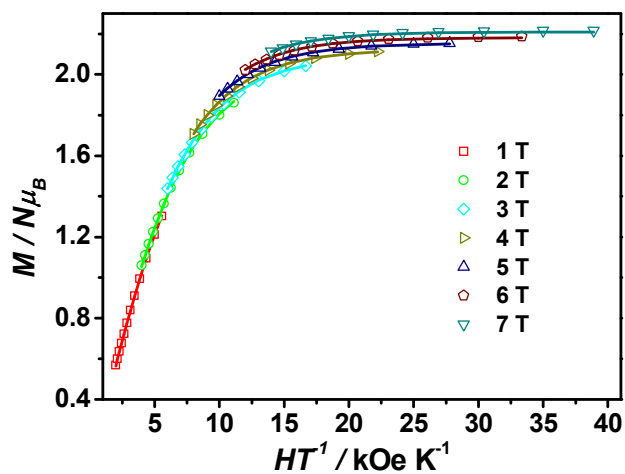


Figure 3. Variable-temperature, variable-field dc magnetization data collected on pure polycrystalline samples of **1** (top) and **2** (bottom). Fields of 1 to 7 T were used from 1.8 to 5 K. Solid lines indicate the best fits with the *PHI* program.¹⁹

The polycrystalline X-band EPR at 4.2 K present rhombic symmetry ($g_{\text{eff}} = [5.20, 4.00, 2.05]$ for **1** and $g_{\text{eff}} = [6.30, 4.08, 2.48]$ for **2**). The patterns of the g_{eff} values are characteristic of an orbitally non-degenerate ground state with a large positive D value (Figures S1 and S2).^[21,5c,5d] HF-EPR spectra were also recorded on the polycrystalline samples of **1** and **2** at the frequency up to 235 GHz in order to further probe their magnetic anisotropies. As the magnitude of D values (35.8 and 35.7 cm^{-1} for **1** and **2**) are out of the frequency range in our measurements ($235 \text{ GHz} \sim 8 \text{ cm}^{-1}$), no any transitions between Kramers doublets $M_S = \pm 1/2$ and $M_S = \pm 3/2$ were observed (Figure 4). Both HF-EPR spectra of **1** and **2** contain three signals, typical for a spin $3/2$ system with large and positive D values.^{5a,5b,5d,5i,20d,22} All signals were from the intra-Kramers transitions within the lowest doublet $M_S = \pm 1/2$ with $\Delta M_S = \pm 1$, which was confirmed by the field versus frequency dependence of the observed turning points (Figure 5).

HF-EPR spectra of **1** and **2** could be well simulated with the estimated D values from SQUID measurements, as shown in Figures 4 and 5. D values are confirmed to be positive. For **1**, the simulation was done using D value obtained by magnetization measurements ($+35.8 \text{ cm}^{-1}$), while adjusting the zero-field splitting parameter E and intrinsic g values, which gave an axial g -tensor [$g_x = g_y = 2.21(1)$, $g_z = 1.98(1)$] and

$|E| = 0.07(1) \text{ cm}^{-1}$ ($|E/D| \sim 0.002$). Similar simulation was also performed on the HFEPR spectrum of **2**. The parameters $D = 35.7 \text{ cm}^{-1}$ (SQUID), $|E| = 1.81(1) \text{ cm}^{-1}$ ($|E/D| \sim 0.051$), $g_x = g_y = 2.21(1)$, and $g_z = 2.00(1)$ were obtained. If the sign of the D values are set to be negative, no reasonably simulated spectrum could be obtained (Figure 4). It should be noted that no transitions between Kramers doublets $M_S = \pm 1/2$ and $M_S = \pm 3/2$ were observed due to the large D values and the limitation of the technique, as shown in several mononuclear Co(II) complexes.^{5a,5b,5d,5i,20d,22} The derived Hamiltonian parameters are not very precise, however, the positive sign of D value has been unambiguously determined, which further demonstrates the easy plane magnetic anisotropies of **1** and **2**.

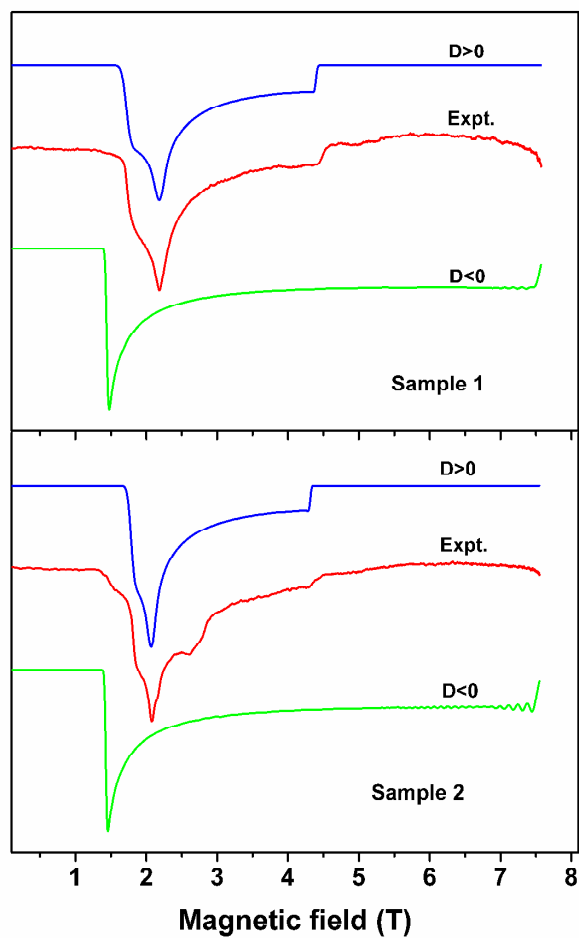


Figure 4. Top: HF EPR spectrum of **1** at 4.2 K (red) and its simulations (blue trace: positive D ; green trace: negative D) at 120 GHz. Bottom: HF EPR spectrum of **2** at 4.2 K (red) and its simulations (blue trace: positive D ; green trace: negative D) at 120 GHz.²³

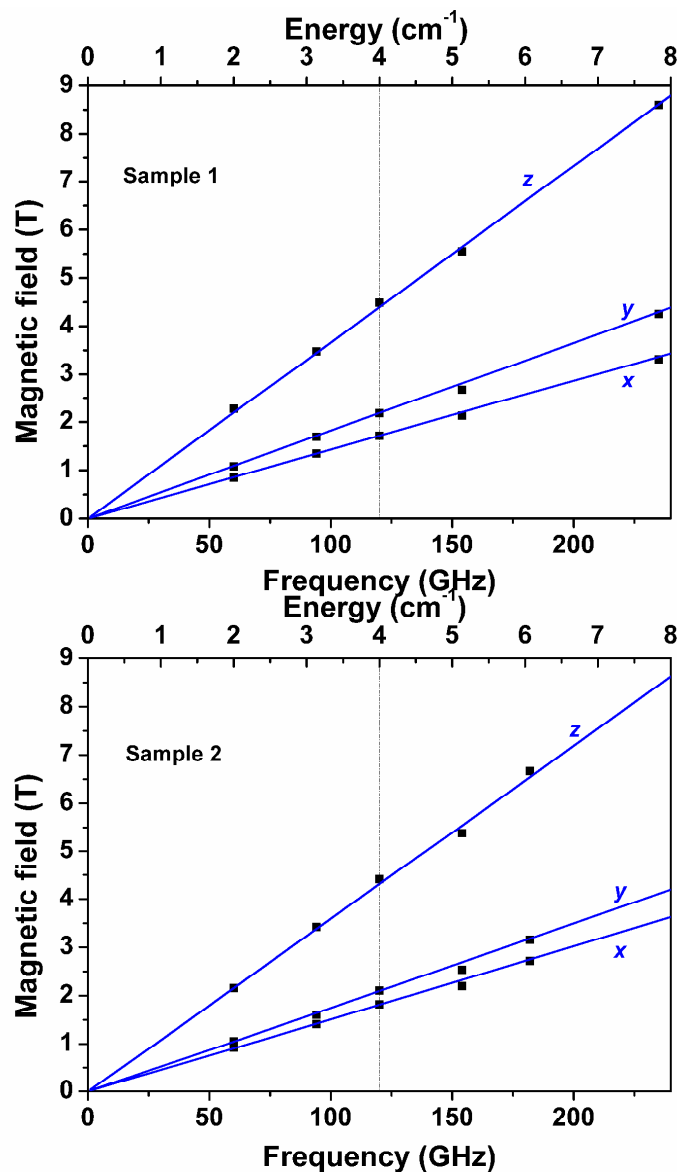


Figure 5. Resonance field vs microwave frequency (quantum energy) for EPR transitions for **1** (top) and **2** (bottom). Simulations were conducted the Hamiltonian parameters used in Figure 4.²³ Solid lines show the (x, y, z) transitions as labeled. The vertical dashed lines represent the frequency (120 GHz) used in Figure 4 at which the spectra were recorded or simulated.

To investigate single molecular magnetism in **1** and **2**, alternative-current (ac)

susceptibility measurements were carried out at 1.8 K under different external dc fields of 0 – 2000 Oe (Figures S3 and S4). Within the frequency range 1-1000 Hz, no out-of phase ac susceptibilities (χ_M'') signals were found for both complexes under zero applied dc field. This is primarily due to the occurrence of the quantum tunneling of the magnetization (QTM) through the spin-reversal barrier, as usually observed for many mononuclear SMMs based on cobalt(II) ion.^{5, 6e-6p} For non-integer spin systems, such as the high-spin cobalt(II) ion with $S = 3/2$, the transverse anisotropy (E) would not promote tunneling through mixing of the ground $\pm m_S$ levels.²⁴ Therefore, the origin of QTM in **1** and **2** could be attributed to the hyperfine and dipolar interactions rather than the transverse anisotropy (E).²⁵ As depicted in Figures S3 and S4, when a small static dc field was applied, the nonzero χ_M'' signals appeared. The χ_M'' signal intensifies with the increase of the applied dc field. At the applied dc field above 1000 Oe for **1** and 1200 Oe for **2**, the maximum begins to move to the high frequency. Therefore, the optimum dc fields of 1000 Oe and 1200 Oe were determined for **1** and **2**, which were used as the applied dc fields to probe the temperature and frequency of the ac susceptibility (Figures 6 and S5-S6). The frequency dependent χ_M'' peaks were observed for **1** at the temperature from 1.8 to 4.6 K with the frequency range 1-1000 Hz while only one maximum was observed for **2**. Obviously the magnetic relaxation is slower in **1** than in **2** in spite of the similar zero field splitting D values.

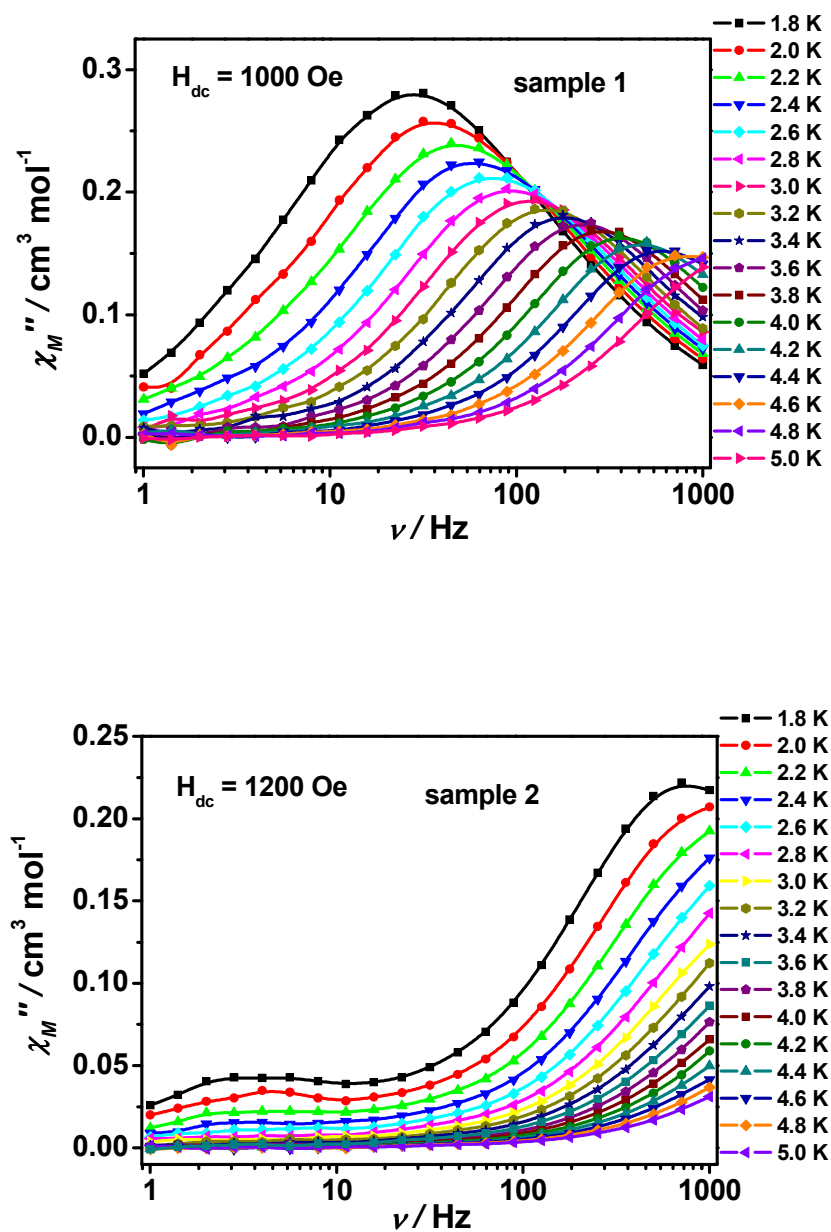


Figure 6. Frequency dependence of the out-of-phase ac magnetic susceptibility from 1 to 1000 Hz under applied dc field of 1.0 KOe for **1** (top) and 1.2 KOe for **2** (bottom). The solid lines are for eye guide.

For **1**, the Cole-Cole plots at different temperature gave semicircular shape,

which were fit using the generalized Debye model²⁶ (Figure S7). The fitting values of χ_T (isothermal susceptibility), χ_S (adiabatic susceptibility), τ (relaxation time) and α (α determines the width of the distribution of relaxation times) are summarized in Table S2 in the *ESI*. The parameters α is in the range of 0.03–0.27 and found to increase with the decrease of the temperature, which suggests that a small distributions of relaxation times. The relaxation times τ extracted from using the χ_M'' peaks from the frequency-dependent data in the temperature from 1.8 to 4.6 K were used to construct the Arrhenius plot shown in Figure S8. A fit to the linear relationship affords an effective energy barrier of $U_{eff} = 17.7 \text{ cm}^{-1}$ with $\tau_o = 7.68 \times 10^{-7} \text{ s}^{-1}$. In the case of **2**, there is only one maximum observed in the frequency-dependence out-of-phase ac magnetic susceptibility signals, as depicted in the bottom of Figure 6. Hence the relaxation times were extracted from the isothermal χ_M'' versus frequency plots using a classical scaling method^{7i,27} (Figure S9). The obtained relaxation time vs. $1/T$ plot is displayed in Figure S10, which give a value of $U_{eff} = 11.0 \text{ cm}^{-1}$ ($\tau_o = 7.01 \times 10^{-7}$) by fitting $\ln(\tau)$ versus $1/T$ in the high-temperature regime. It should be noted that such an estimation of effective energy barrier is based on the frequently made assumption of a thermally assisted Orbach process²⁸ and a temperature-independent QTM as dominant relaxation processes. In fact, it has been demonstrated in some cases that the Orbach mechanism is not necessarily the dominant process at least in the investigated temperature range^{.5d,5e,7k,29-31}

The sizes of effective energy barrier of $U_{eff} = 17.7 \text{ cm}^{-1}$ for **1** and $U_{eff} = 11.0 \text{ cm}^{-1}$ for **2** are not comparable with the $2D$ values expected for an Orbach process. Such a

thermal-assisted process was suggested by Long et al^{5a} as the dominant relaxation process in the first tetrahedral Co(II)-SIM with the easy plane anisotropy. In the suggested process, the direct relaxation between the ground $M_S = \pm 1/2$ levels in tetrahedral cobalt(II) complex with easy-plane anisotropy ($D > 0$) is slowed due to the phonon bottleneck, generating the Orbach process through the excited $M_S = \pm 3/2$ levels, with the observed barrier consistent with the $2D$ values.^{5a} In some other cobalt(II)-SIMs^{5b-5c}, the transverse anisotropy (E) instead of the axis anisotropy (D) was suggested as the possible source facilitating the occurrence of slow magnetic relaxation behavior. In this sense, a possible axis within the xy plane would be constructed by the transverse anisotropy. The energy of the transverse barrier for rotation of the magnetic moment in the xy plane could be $\Delta U = |E|(S^2 - 1/4)$ for a half-integral spin. However, the values of U_{eff} (17.7 cm^{-1} and 11.0 cm^{-1}) obtained experimentally from ac susceptibility measurements are significantly larger than the expected energy barrier $|E|(S^2 - 1/4)$ associated with the in-plane anisotropy. This inconsistency suggests this interpretation based on the transverse anisotropy is incompatible with the system of **1** and **2**, and was also rejected in other reports.^{5d-5e}

The curvature found in the Arrhenius plots of **1** and **2** implies a non-negligible direct and/or Raman processes in determining the relaxation rate. Therefore a model including three possible relaxation processes. *i.e.* direct, Raman and Orbach mechanisms³² were employed to analyze the contribution to the relaxation in **1** by using equation (1):

$$\tau^{-1} = AT + CT^n + \tau_0^{-1} \exp(-U_{eff} / kT) \quad (1)$$

where the terms in equation (1) represent the contributions of direct, Raman or Raman-like and Orbach mechanisms. For the second term, $n = 7$ expected for the Raman process in non-Kramers ion and $n = 9$ for Kramers ion while $n = 1-6$ can occur for optical acoustic Raman-like process.³²⁻³³ The best fits were obtained and summarized in Table 3. As depicted in Figure S11, the fit reproduce the experimental data very well. For **1**, it is concluded that the contributions of Orbach and direct processes are very small compared with the Raman process. Furthermore, if the two contributions of the Orbach and direct processes are neglected, the relaxation time data can be modeled by a power law $\tau^{-1} = CT^n$ with the resulting value $C = 17.8 \text{ K}^{-3}$ and $n = 3.5$ (Figure 7). These fits suggest that the optical acoustic Raman-like mechanism ($n = 3.5$) is the dominant process in the magnetic relaxation of **1**. In the case of **2**, the region at low temperature (1.8 – 2.8 K) is dominated by a direct process, whereas the relaxation process at high temperature (2.8 – 5 K) mainly attribute to the optical acoustic Raman-like mechanism (Figure S12). Such Raman or Raman-like mechanism has been demonstrated to occur in the dynamic magnetic relaxation of some SIMs with the easy plane anisotropy including six-coordinate Co(II) SIM [Co(acac)₂(H₂O)₂] ($n = 9$),^{5e} Y-Co(II) SIM ($n = 4.5$),^{5d} and two-coordinate Fe(I) SIM ($n = 8.14$).^{7k}

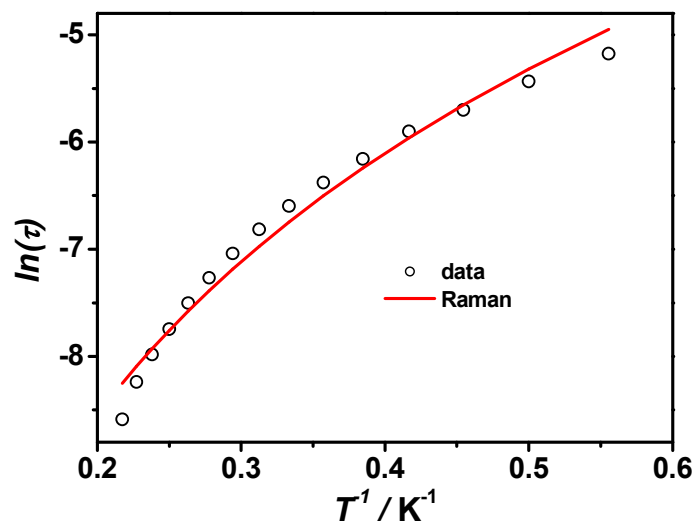


Figure 7. Temperature dependence of the magnetization relaxation rates of **1**. The solid red lines represent only the Raman process was employed to fit.

Table 3. Summary of the parameters of direct, Raman, and Orbach relaxation for **1** and **2**.

	H_{dc} (KOe)	n	A ($K^{-1} s^{-1}$)	C ($K^{-4} s^{-1}$)	τ_o (s^{-1})	U_{eff} (cm^{-1})
1	1.0	4.1	60.2	6.5	7.5×10^{-10}	41.7
	0.5	2.8	0.0575	58.9	3.7×10^{-9}	36.8
2	1.2	3.6	2071.0	126.8	8.5×10^{-8}	24.5
	0.5	3.5	315.2	508.0	9.1×10^{-8}	20.2
Zn-1	1.0	8.17	1.88	0.00138	1.8×10^{-14}	95.0

Additional ac susceptibility measurements under an applied dc field of 500 Oe

were also performed in the temperature range of 1.8-10 K for **1** and **2**. The temperature- and frequency- dependence of the ac susceptibility are depicted in Figure S13 and S14. Similar with the dynamic magnetic behaviors observed under the applied dc fields of 1.0 KOe (1.2 KOe), several maximums of χ_M'' signals at the temperature from 1.8 to 4.2 K for **1** and only one peak for **2** were observed in the frequency range 1-1000 Hz. Similar treatments were used to extract the relaxation rates occurring in **1** and **2**, which were analyzed using equation (1) involving the three possible relaxation processes. *i.e.* direct, Raman and Orbach mechanisms³² (see Figures S15-S17). These analyses revealed that the optical acoustic Raman-like mechanism is dominant in **1** and **2** over the studied temperature range with the applied dc field of 500 Oe (Figures S15 and S17)

In order to investigate the effect of intermolecular interactions in the magnetic relaxation of **1**, a magnetically dilute sample $[\text{Co}_{0.1}\text{Zn}_{0.9}(\text{L})_3(\text{NO}_3)_2]$ (L = 4-*tert*-butylpyridine, **Zn-1**) was prepared by co-crystallization. The dc field of 1000 Oe was applied during the ac measurement for **Zn-1**. The Arrhenius plot derived from the peaks of out-of-phase χ_M'' from the frequency-dependent data for **Zn-1** (Figure S18) was analyzed by using eqn (1), yielding the parameters given in Table 3. Comparison between Figures S11 and S19 and the parameters in Table 3 could give us two conclusions: (a) The contributions of Orbach and direct processes are not significant in both cases. The dominant pathway is Raman or Raman-like process. (b) The difference between the diluted and undiluted samples is the n value. The derived n value is 8.17 for sample **Zn-1** while $n = 4.1$ for **1**. This suggests that after the

dilution, the main process become Raman process in contrast with the optical acoustic Raman-like process in **1**.

In summary, we have reported the syntheses, structures, and magnetic properties of two seven-coordinate cobalt(II) complexes with easy plane anisotropy. The magnetization data reveal the large and positive values of the zero-field splitting parameters (D) and very small value of the transverse anisotropy (E), which were confirmed by HFEPR data. Both complexes show the slow magnetic relaxation behavior in the presence of an applied dc field. The dominant Raman-like process is applied to explain the dynamic magnetic behaviors of **1**. For **2**, the relaxation at high temperature region can occur via Raman-like process while a direct process become the dominant mechanism at lower temperature range.

Acknowledgments

We are grateful for the financial support from the National Basic Research Program of China (No. 2013CB922102 to X.-T.C and Y. S.), the Natural Science Grant of China (No. 21471078 to X.-T.C), and the U.S. National Science Foundation (CHE-1362548 to Z.-L.X).

References

- 1 (a) D. Gatteschi, R. Sessoli and J. Villain, *Molecular Nanomagnets*, Oxford University Press, Oxford, 2006; (b) D. Gatteschi and R. Sessoli, *Angew. Chem.*,

- Int. Ed.* 2003, **42**, 268; (c) W. Wernsdorfer and R. Sessoli, *Science*, 1999, **284**, 133; (d) M. N. Leuenberger and D. Loss, *Nature*, 2001, **410**, 789; (e) L. Bogani and W. Wernsdorfer, *Nat. Mat.*, 2008, **7**, 179.
- 2 (a) G. Aromí and E. K. Brechin, in *Struct. Bonding*, ed. R. Winpenny, Springer-Verlag, Berlin Heidelberg, **2006**, vol. 122, pp. 1-67; (b) R. Winpenny, *Molecular Cluster Magnets*, World Scientific, Singapore, 2012; (c) G. Christou, *Polyhedron*, 2005, **24**, 2065; (d) R. Bagai and G. Christou, *Chem. Soc. Rev.*, 2009, **38**, 1011; (e) D. Gatteschi, R. Sessoli and A. Cornia, *Chem. Commun.* 2000, **9**, 725; (f) M. Murrie, *Chem. Soc. Rev.*, 2010, **39**, 1986; (f) K. S. Pedersen, J. Bendix and R. Clérac, *Chem. Commun.*, 2014, **50**, 4396.
- 3 (a) R. Sessoli and A. K. Powell, *Coord. Chem. Rev.* 2009, **253**, 2328; (b) Y. N. Guo, G. F. Xu, Y. Guo and J. K. Tang, *Dalton Trans.*, 2011, **40**, 9953; (c) P. Zhang, Y. N. Guo and J. K. Tang, *Coord. Chem. Rev.*, 2013, **257**, 1728; (d) F. Habib and M. Murugesu, *Chem. Soc. Rev.*, 2013, **42**, 3278.
- 4 (a) N. Ishikawa, M. Sugita, T. Ishikawa, S. Koshihara and Y. Kaizu, *J. Am. Chem. Soc.*, 2003, **125**, 8694; (b) D. N. Woodruff, R. E. P. Winpenny and R. A. Layfield, *Chem. Rev.*, 2013, **113**, 5110.
- 5 (a) J. M. Zadrozny, J. J. Liu, N. A. Piro, C. J. Chang, S. Hill and J. R. Long, *Chem. Comm.*, 2012, **48**, 3897; (b) D. Y. Wu, X. X. Zhang, P. Huang, W. Huang, M. Y. Ruan and Z. W. Ouyang, *Inorg. Chem.*, 2013, **52**, 10976; (c) J. Vallejo, I. Castro, R. Ruiz-García, J. Cano, M. Julve, F. Lloret, G. D. Munno, W. Wernsdorfer and E. Pardo, *J. Am. Chem. Soc.*, 2012, **134**, 15704; (d) E. Colacio, J.

- Ruiz, E. Ruiz, E. Cremades, J. Krzystek, S. Carretta, J. Cano, T. Guidi, W. Wernsdorfer and E. K. Brechin, *Angew. Chem., Int. Ed.*, 2013, **52**, 9130; (e) S. Gómez-Coca, A. Urtizberea, E. Cremades, P. J. Alonso, A. Camón, E. Ruiz and F. Luis, *Nat. Comm.*, 2014, **5:4300**, 1; (f) R. Herchel, L. Váhovská, I. Potočňák and Z. Trávníček, *Inorg. Chem.*, 2014, **53**, 5896; (g) S. Gomez-Coca, E. Cremades, N. Aliaga-Alcalde and E. Ruiz. *J. Am. Chem. Soc.*, 2013, **135**, 701; (h) C. Rajnák, J. Titiš, O. Fuhr, M. Ruben and R. Boča, *Inorg. Chem.* 2014, **53**, 8200; (i) W. Huang, T. Liu, D. Y. Wu, J. J. Cheng, Z. W. Ouyang and C. Y. Duan, *Dalton Trans.*, 2013, **42**, 15326; (j) X. C. Huang, C. Zhou, D. Shao and X.-Y. Wang, *Inorg. Chem.*, 2014, **53**, 12671.
- 6 (a) J. M. Zadrozny and J. R. Long, *J. Am. Chem. Soc.*, 2011, **133**, 20732; (b) J. M. Zadrozny, J. Telser and J. R. Long, *Polyhedron*, 2013, **64**, 209; (c) Y. -Y. Zhu, C. Cui, Y. -Q. Zhang, J. -H. Jia, X. Guo, C. Gao, K. Qian, S. -D. Jiang, B. -W. Wang, Z. -M. Wang and S. Gao, *Chem. Sci.*, 2013, **4**, 1802; (d) M. S. Fataftah, J. M. Zadrozny, D. M. Rogers and D. E. Freedman, *Inorg. Chem.*, 2014, **53**, 10716; (e) F. Yang, Q. Zhou, Y. Q. Zhang, G. Zeng, G. H. Li, Z. Shi, B. W. Wang and S. H. Feng, *Chem. Comm.*, 2013, **49**, 5289; (f) D. K. Cao, J. Q. Feng, M. Ren, Y. W. Gu, Y. Song and M. D. Ward, *Chem. Comm.*, 2013, **49**, 8863; (g) F. Habib, O. R. Luca, V. Vieru, M. Shiddiq, I. Korobkov, S. I. Gorelsky, M. K. Takase, L. F. Chibotaru, S. Hill, R.H. Crabtree and M. Murugesu, *Angew. Chem., Int. Ed.*, 2013, **52**, 11290; (h) T. Jurca, A. Farghal, P.-H. Lin, I. Korobkov, M. Murugesu and D. S. Richeson, *J. Am. Chem. Soc.*, 2011, **133**, 15814; (i) V. Chandrasekhar,

- A. Dey, A. J. Mota and E. Colacio, *Inorg. Chem.*, 2013, **52**, 4554; (j) A. Buchholz, A. O. Eseola and W. Plass, *C. R. Chim.*, 2012, **15**, 929; (k) A. Eichhofer, Y. Lan, V. Mereacre, T. Bodenstern and F. Weigend, *Inorg. Chem.*, 2014, **53**, 1962; (l) R. Boča, J. Miklovič and J. Titiš, *Inorg. Chem.*, 2014, **53**, 2367; (m) P. Cucos, F. Tuna, L. Sorace, I. Matei, C. Maxim, S. Shova, R. Gheorghe, A. Caneschi, M. Hillebrand and M. Andruh, *Inorg. Chem.*, 2014, **53**, 7738; (n) M. R. Saber and K. R. Dunbar, *Chem. Commun.*, 2014, **50**, 12266; (o) L. Chen, J. Wang, J. -M. Wei, W. Wernsdorfer, X. -T. Chen, Y. -Q. Zhang, Y. Song and Z. -L. Xue, *J. Am. Chem. Soc.*, 2014, **136**, 12213; (p) C. Plenk, J. Krause and E. Rentschler, *Eur. J. Inorg. Chem.*, 2015, 370.
- 7 (a) J. M. Zadrozny, D. J. Xiao, M. Atanasov, G. J. Long, F. Grandjean, F. Neese and J. R. Long, *Nat. Chem.*, 2013, **5**, 577; (b) J. M. Zadrozny, M. Atanasov, A. M. Bryan, C.-Y. Lin, B. D. Reken, P. P. Power, F. Neese and J. R. Long, *Chem. Sci.*, 2013, **4**, 125; (c) M. Atanasov, J. M. Zadrozny, J. R. Long and F. Neese, *Chem. Sci.*, 2013, **4**, 139; (d) P.-H. Lin, N. C. Smythe, S. I. Gorelsky, S. Maguire, N. J. Henson, I. Korobkov, B. L. Scott, J. C. Gordon, R. T. Baker and M. Murugesu, *J. Am. Chem. Soc.*, 2011, **133**, 15806; (e) D. E. Freedman, W. H. Harman, T. D. Harris, G. J. Long, C. J. Chang and J. R. Long, *J. Am. Chem. Soc.*, 2010, **132**, 1224; (f) W. H. Harman, T. D. Harris, D. E. Freedman, H. Fong, A. Chang, J. D. Rinehart, A. Ozarowski, M. T. Sougrati, F. Grandjean, G. J. Long, J. R. Long and C. J. Chang, *J. Am. Chem. Soc.*, 2010, **132**, 18115; (g) D. Weismann, Y. Sun, Y. Lan, G. Wolmershäuser, A. K. Powell and H. Sitzmann, *Chem. Eur. J.*, 2011, **17**,

- 4700; (h) C. Mathonière, H.-J. Lin, D. Siretanu, R. Clérac and J. M. Smith, *J. Am. Chem. Soc.*, 2013, **135**, 19083; (i) X. Feng, C. Mathonière, I.-R. Jeon, M. Rouzières, A. Ozarowski, M. L. Aubrey, M. I. Gonzalez, R. Clérac and J. R. Long, *J. Am. Chem. Soc.*, 2013, **135**, 15880; (j) S. Mossin, B. L. Tran, D. Adhikari, M. Pink, F. W. Heinemann, J. Sutter, R. K. Szilagyi, K. Meyer and D. J. Mindiola, *J. Am. Chem. Soc.*, 2012, **134**, 13651; (k) P. P. Samuel, K. C. Mondal, N. Amin Sk, H. W. Roesky, E. Carl, R. Neufeld, D. Stalke, S. Demeshko, F. Meyer, L. Ungur, L. F. Chibotaru, J. Christian, V. Ramachandran, J. van Tol and N. S. Dalal, *J. Am. Chem. Soc.*, 2014, **136**, 11964.
- 8 R. C. Poulten, M. J. Page, A. G. Algarra, J. J. Le Roy, I. Lopez, E. Carter, A. Llobet, S. A. Macgregor, M. F. Mahon, D. M. Murphy, M. Murugesu and M. K. Whittlesey, *J. Am. Chem. Soc.*, 2013, **135**, 13640.
- 9 (a) R. Ishikawa, R. Miyamoto, H. Nojiri, B. K. Breedlove and M. Yamashita, *Inorg. Chem.*, 2013, **52**, 8300; (b) A. Grigoropoulos, M. Pissas, P. Papatolis, V. Psycharis, P. Kyritsis and Y. Sanakis, *Inorg. Chem.*, 2013, **52**, 12869; (c) J. Vallejo, A. Pascual-Álvarez, J. Cano, I. Castro, M. Julve, F. Lloret, J. Krzystek, G. De Munno, D. Armentano, W. Wernsdorfer, R. Ruiz-García and E. Pardo, *Angew. Chem., Int. Ed.*, 2013, **52**, 14075; (d) G. A. Craig, J. J. Marbey, S. Hill, O. Roubeau, S. Parsons, and M. Murrie, *Inorg. Chem.*, 2015, **54**, 13; (e) L. Chen, J. Wang, Y.-Z. Liu, Y. Song, X.-T. Chen, Y.-Q. Zhang and Z.-L. Xue, *Eur. J. Inorg. Chem.*, 2015, 271.
- 10 (a) J. Martinez-Lillo, T. F. Mastropietro, E. Lhotel, C. Paulsen, J. Cano, G. De

- Munno, J. Faus, F. Lloret, M. Julve, S. Nellutla and J. Krzystek, *J. Am. Chem. Soc.*, 2013, **135**, 13737; (b) K. S. Pedersen, M. Sigrist, M. A. Soensen, A.-L. Barra, T. Weyhermuller, S. Piligkos, C. A. Thuesen, M. G. Vinum, H. Mutka, H. Weihe, R. Clerac and J. Bendix, *Angew. Chem., Int. Ed.*, 2014, **53**, 1351.
- 11 M. Dey and N. Gogoi, *Angew. Chem., Int. Ed.*, 2013, **52**, 12780.
- 12 P. P. Power, *Chem. Rev.*, 2012, **112**, 3482.
- 13 SMART & SAINT Software Reference Manuals, version 6.45; Bruker Analytical X-ray Systems, Inc.: Madison, WI, 2003.
- 14 G. M. Sheldrick, SADABS: Software for Empirical Absorption Correction, version 2.05; University of Göttingen: Göttingen, Germany, 2002.
- 15 G. M. Sheldrick, SHELXL97: Program for Crystal Structure Refinement; University of Göttingen: Göttingen, Germany, 1997.
- 16 (a) S. L. Wang, L. Li, Z. W. Ouyang, Z. C. Xia, N. M. Xia, T. Peng and K. B. Zhang, *Acta Phys. Sin.*, 2012, **61**, 107601; (b) H. Nojiri and Z. W. Ouyang, *Terahertz Sci. Technol.*, 2012, **5**, 1.
- 17 C. C. Addison, N. Logan and S. C. Wallwork, *Quart. Rev.*, 1971, **25**, 289.
- 18 (a) S. Alvarez, P. Alemany, D. Casanova, J. Cirera, M. Llunell and D. Avnir, *Coord. Chem. Rev.*, 2005, **249**, 1693; (b) D. Casanova, P. Alemany, J. M. Bofill and S. Alvarez, *Chem. Eur. J.*, 2003, **9**, 6.
- 19 N. F. Chilton, R. P. Anderson, L. D. Turner, A. Soncini and K. S. Murray, *J.*

- Comput. Chem.*, 2013, **34**, 1164.
- 20 (a) C. Platas-Iglesias, L. Vaiana, D. Esteban-Gómez, F. Avecilla, J. A. Real, A. de Blas and T. Rodríguez-Blas, *Inorg. Chem.*, 2005, **44**, 9704; (b) L. J. Batchler, M. Sangalli, R. Guillot, N. Guihéry, R. Maurice, F. Tuna and T. Mallah, *Inorg. Chem.*, 2011, **50**, 12045; (c) F. Schleife, A. Rodenstein, R. Kirmse and B. Kersting, *Inorg. Chim. Acta*, 2011, **374**, 521; (d) R. Ruamps, L. J. Batchelor, R. Maurice, N. Gogoi, P. Jiménez-Lozano, N. Guihéry, C. de Graaf, A. -L. Barra, J. -P. Sutter and T. Mallah, *Chem. Eur. J.*, 2013, **19**, 950.
- 21 L. Banci, A. Bencini, C. Benelli, D. Gatteschi and C. Zanchini, *Struct. Bonding*, 1982, **52**, 37.
- 22 F. R. Xavier, A. Neves, A. Casellato, R. A. Peralta, A. J. Bortoluzzi, B. Szpoganicz, P. C. Severino, H. Terenzi, Z. Tomkowicz, S. Ostrovsky, W. Haase, A. Ozarowski, J. Krzystek, J. Telser, G. Schenk and L. R. Gahan, *Inorg. Chem.*, 2009, **48**, 7905
- 23 Simulations were performed using SPIN developed by Andrew Ozarowski in National High Magnetic Field Laboratory, US.
- 24 H. A. Kramers, *Proc. R. Acad. Sci. Amsterdam*, 1930, **33**, 959.
- 25 N. Ishikawa, M. Sugita and W. Wernsdorfer, *J. Am. Chem. Soc.*, 2005, **127**, 3650; (b) N. Ishikawa, M. Sugita and W. Wernsdorfer, *Angew. Chem., Int. Ed.*, 2005, **44**, 2931.
- 26 (a) K. S. Cole and R. H. Cole, *J. Chem. Phys.*, 1941, **9**, 341; (b) S. M. J. Aubin, Z.

- M. Sun, L. Pardi, J. Krzystek, K. Folting, L. C. Brunel, A. L. Rheingold, G. Christou and D. N. Hendrickson, *Inorg. Chem.*, 1999, **38**, 5329.
- 27 (a) A. Labarta, O. Iglesias, L. Balcells and F. Badia, *Phys. Rev. B*, 1993, **48**, 10240; (b) D. M. Piñero Cruz, D. N. Woodruff, I.-R. Jeon, I. Bhowmick, M. Secu, E. A. Hillard, P. Dechambenoit and Rodolphe Clérac, *New J. Chem.*, 2014, **38**, 3443.
- 28 R. Orbach, *Proc. R. Soc. London, Ser. A*, 1961, 264, 458.
- 29 J.-L. Liu, K. Yuan, J.-D. Leng, L. Ungur, W. Wersdorfer, F.-S. Guo, L. F. Chibotaru and M.-L. Tong, *Inorg. Chem.*, 2012, 51, 8538.
- 30 E. Lucaccini, L. Sorace, M. Perfetti, J.-P. Costes and R. Sessoli, *Chem. Commun.*, 2014, 50, 1648.
- 31 K. S. Pedersen, L. Ungur, M. Sigrist, A. Sundt, M. Schau-Magnussen, V. Vieru, H. Mutka, S. Rols, H. Weihe, O. Waldmann, L. F. Chibotaru, J. Bendix and J. Dreiser, *Chem. Sci.*, 2014, 5, 1650.
- 32 R. L. Carlin, A. J. van Duyneveldt, *Magnetic Properties of Transition Metal compounds*, Springer-Verlag, New York, 1976.
- 33 K. N. Shrivastava, *Phys. Status Solidi B*, 1983, **117**, 437.

Slow magnetic relaxation in mononuclear seven-coordinate cobalt(II) complexes with easy plane anisotropy

Lei Chen, Shu-Yang Chen, Yi-Chen Sun, Yu-Mei Guo, Xue-Tai Chen, Zhenxing Wang,

Z. W. Ouyang, You Song, and Zi-Ling Xue

Two mononuclear pentagonal bipyramid cobalt(II) complexes with the positive zero-field splitting D values are demonstrated to exhibit field-induced slow relaxation behaviour.

